Ultra-broad molecular weight distribution effects on viscoelastic properties of linear multimodal PE

Levente Szántó,[1,a)] Yukang Feng,[1,b)] Fan Zhong,[1,c)] Timo Hees,[1,d)] Evelyne van Ruymbeke,[2,e)] Rolf Mülhaupt,[1,f)] and Christian Friedrich[1,g)]

[1]*Freiburg Materials Research Center (FMF), Albert-Ludwigs-University of Freiburg, Stefan-Meier-Street 21, D-79104 Freiburg, Germany and Institute for Macromolecular Chemistry, Albert-Ludwigs-University of Freiburg, Stefan-Meier-Street 31, D-79104 Freiburg, Germany*
[2]*Bio- and Soft Matter (BSMA), Institute of Condensed Matter and Nanosciences, Université Catholique de Louvain, Croix du Sud 1, Louvain-la-Neuve B-1348, Belgium*

(Received 9 May 2019; final revision received 10 July 2019; published 30 July 2019)

Abstract

Rheological investigation of polyethylene (PE) blends with a significant amount (up to 50 wt. %) of ultrahigh molecular weight PE (UHMWPE, with weight average molecular weight $M_w > 10^6$ g/mol) was not accessible so far. The development of special Enders catalysts allows the synthesis of such homogeneous PE reactor blends (RBs). In this paper, by melt blending of RBs with high-density PE polymer matrix, multimodal PE blends were prepared and their rheological properties were investigated. The analysis grants access to better understand how notably high amount of UHMWPE and ultra-broad molecular weight distribution displaying extremely high polydispersity, $Đ \sim 1000$, influence the linear viscoelasticity. Moreover, taking advantage of the opportunities offered by molecular models, applying the tube-based time-marching algorithm, the "rheological" molecular weight distribution (MWD) of multimodal PE blends was determined, overcoming drawbacks of high-temperature size exclusion chromatography. Analyzing the zero-shear viscosity, η_0, versus M_w scaling relation for blends of any MWD, a correction scheme was developed which allows to take into account the $Đ$ effects on η_0 properly. The analysis revealed that in a double logarithmic plot versus M_w, corrected η_0 shows a unique linear dependency with a slope of 3.6 if M_w is smaller than the reptation molecular weight (M_r). If $M_w > M_r$, the slope of this linear dependency turns into 3. The analysis of transition zone between the two linear dependencies allowed the experimental determination of PEs M_r. © *2019 The Society of Rheology.* https://doi.org/10.1122/1.5109481

I. INTRODUCTION

Polyolefins, among them polyethylene (PE), represent the largest amount of worldwide produced polymeric materials, possessing vast applicability [1]. Due to their broad applicability, there is an urge to improve PE manufacturing, processing, and mechanical properties further. The breakthroughs of the polymer synthesis in the last few decades allowed the tailoring of polyolefins by controlling the molecular weight (MW), molecular weight distribution (MWD), topology, etc. [2]. For example, PE with broad MWD shows good slow crack growth- and impact resistance and improved processability [3]. Furthermore, the presence of low MW components shifts the appearance of different processing defects to higher shear rates, increasing the productivity [4–6]. In addition, ultrahigh molecular weight PE (UHMWPE), consisting of chains with weight average molecular weight (M_w) higher than 10^6 g/mol, lends increased tensile strength, toughness, and abrasion and fatigue resistance [7–9]. Thus, through tailored MW and MWD notable material improvements can be achieved. In the past, several attempts were made in order to obtain PE blends, combining the benefits of UHMWPE and high-density PE (HDPE) [10,11]. Due to the high entanglement density and high number of entanglements per chain, the UHMWPE possesses extraordinary high zero-shear viscosity (η_0). Boscoletto *et al.* showed that applying melt blending, only about 3 wt. % of UHMWPE can be dissolved within the HDPE polymer matrix and higher concentrations drive to inhomogeneous blends [10]. Nonetheless, with the help of novel multiple single-site catalysts, Kurek *et al.* synthesized tailor-made trimodal (low molecular weight waxes/HDPE/UHMWPE) polyethylene reactor blends (RBs) with ultra-broad MWD, extraordinarily high polydispersity ($Đ = M_w/M_n$), and incorporating up to 16 wt. % of UHMWPE without ceding the melt processability and homogeneity [12]. The access to these catalysts and adjusting the catalyst support grant the possibility to melt compound bimodal RBs and commercial HDPE. The resulting homogeneous trimodal PE blends with significantly increased UHMWPE content combine excellent processability and outstanding mechanical properties [13,14]. In addition, Zhong *et al.* synthetized bimodal PE (Wax/UHMWPE) RB containing 40 wt. % of UHMWPE, possessing a $Đ$ of about 1000. Consequently, via melt blending they incorporated up to 32 wt. % of UHMWPE into a commercial HDPE without considerably reducing processability [15,16].

[a)]Electronic mail: levente.szanto@fmf.uni-freiburg.de
[b)]Electronic mail: fyk8874@icloud.com
[c)]Electronic mail: fan.zhong@fmf.uni-freiburg.de
[d)]Electronic mail: timo.hees@fmf.uni-freiburg.de
[e)]Electronic mail: evelyne.vanruymbeke@uclouvain.be
[f)]Electronic mail: rolf.muelhaupt@makro.uni-freiburg.de
[g)]Author to whom correspondence should be addressed; electronic mail: christian.friedrich@fmf.uni-freiburg.de

© 2019 by The Society of Rheology, Inc.

In order to optimize the processing conditions, rheological measurements are crucial. It is well known that MW, MWD, and topology strongly affect the linear viscoelasticity (LVE) of entangled polymer [1,17–19]. For example, η_0 increases with M_w strongly. The dependence of η_0 on M_w of linear, entangled polymers is reflected by the following equation:

$$\eta_0 = K \cdot M_w^{\alpha}, \tag{1}$$

where K is a temperature and a material dependent parameter, α is equal to 1 for unentangled linear polymers ($M_w < M_c$, where M_c is the critical molecular weight that is approximately two times the entanglement molecular weight M_e [17,20]), and α lays between 3.4 and 3.6 if $M_w > M_c$ but smaller than M_r (reptation molecular weight, $M_r \sim 220M_c$) [21–23]. Last but not least, α is equal to 3 if $M_w > M_r$ [23,24]. Furthermore, the LVE is crucially influenced by the broadness of the polymer MWD. Particularly, an increased $Đ$ causes an earlier onset of the shear thinning behavior, raises the degree of shear thinning, and increases the flow activation energy (E_a) [17,18]. Moreover, the effect of MWD is reflected in the zero-shear viscosity. Albeit, in this context are some contradictory reports. Stadler *et al.* [25], based on the analysis of several linear HDPE, stated that the influence of MWD, if any, is so small that they were not able to determine it even with modern techniques. Nevertheless, Hatzikiriakos revealed that the η_0 of PE with broad MWD exhibit higher values compared to polymers with the same M_w but narrower MWD [18]. Additionally, Ansari *et al.* showed that not only the polydispersity but also the higher moment of the molar mass, like the z-average molecular weight (M_z), strongly affect the zero-shear viscosity [19]. Thus, the presence of high molecular weight species significantly influences the LVE of polymer melts [26–28]. Recently, Wingstrand *et al.* analyzed the rheological behavior of HDPE blends containing 1 wt. % of UHMWPE. They observed that the presence of extremely long chains in the blends, due to their extraordinarily long terminal relaxation time (τ_d), leads to the appearance of a plateau in the flow region. Furthermore, this plateau could be monitored with the help of complementary measurements (creep or stress relaxation analysis) [28].

Due to the fact that ordinary HDPE blends with more than 3 wt. % UHMWPE are heterogeneous, there are, to the best of our knowledge, no rheological investigations related to PE blends containing significantly higher amount of UHMWPE and characterized by ultra-broad MWD.

The presence of extremely long chains poses challenges in the determination of M_w and MWD by high-temperature size exclusion chromatography (HT-SEC) [1,29,30]. In addition, the incidental degradation during sample preparation and the shear degradation of the large structures at the course of measurement lead to erroneous results [31]. This drives the search of key alternatives for MWD determination.

The extensive development of the polymer dynamics theory in the last few decades (e.g., Doi and Edwards [32] or Milner–McLeish [33] theories) enabled to quantitatively describe the LVE of linear polymers [32,34]. It was found that models based on these theories allow the accurate determination of MWD. These models were validated for the polymers with relatively narrow distribution or with low polydispersity. However, quantitative prediction of LVE of blends containing linear polymers characterized by extremely high $Đ$ and multimodal distribution are challenging.

In this study, we report on rheological characterization of multimodal PE blends with extremely high polydispersity ($Đ \approx 1000$) and up to 50 wt. % of UHMWPE content. Moreover, we compare the molecular weights of the multimodal PE blends gathered from HT-SEC with the values from molecular modeling of the rheological data using time-marching algorithm (TMA). Furthermore, we investigate the influence of M_w and MWD on the zero-shear viscosity. This work unveils how multimodal distribution and extremely high molecular weight species resulting in an extremely high $Đ$ affect the LVE of linear PE blends. Additionally, by pushing the boarders, we are challenging the TMA molecular modeling. Moreover, the access to the zero-shear viscosity of polyolefins with very high M_w lets us to experimentally determine the PEs reptation molecular weight (M_r).

II. EXPERIMENTAL

A. Materials and sample preparation

A commercial HDPE, namely, Hostalen GC7260 (LyondellBasell) served as a polymer matrix. The bimodal reactor blends (RBx, where x represents the wt. % of UHMWPE) were synthesized according to a synthesis route detailed elsewhere [15,16]. HDPE, RBx, and 0.5 wt. % of stabilizer (Irganox1010Irgafos 168 = 1:1) were melt blended for 2 min at 200 °C, using a co-rotating twin-screw micro compounder (Xplore™, *DSM*). The RBx content was varied from 0 up to 50 wt. %. The thus produced trimodal PE blends were named, for example, as 10RB40 which designates that 10 wt. % RB40 was melt blended with 89.5 wt. % HDPE and 0.5 wt. % stabilizer. A comprehensive summary regarding sample composition and sample naming is presented in the supplementary material (Table S1) [72]. After melt blending, the resulting strands were quenched in icy water and granulated. The granules were dried under vacuum overnight at 60 °C. Subsequently, platelike samples were prepared at 200 °C and 15 bar using a vacuum hot melt press (P200, Collin).

B. Rheological analysis

The rheological characterization of trimodal PE blends was performed on a stress-controlled MCR301 (Anton Paar) rheometer, using the parallel-plate geometry. The diameter of the sample was 25 mm, and its height was approximately 1 mm. For the samples with more than 30 wt. % RBx content, the 8 mm disks were used. Reducing the diameter of the samples was necessary to avoid tool compliance. Frequency sweeps and creep measurements were conducted at various temperatures ranging from 240 to 130 °C, within the linear viscoelastic regime. Protective nitrogen atmosphere was employed to prevent sample degradation. The obtained isotherms were shifted horizontally to master curves using the shifting program IRIS RHEO-HUB [35]. Furthermore, during the

shifting procedure, in order to obtain master curves the usage of vertical shifting was not necessary. The creep measurements were performed at 190 and 200 °C. The applied shear stress ranges between 50 and 200 Pa (all stresses within the linear viscoelastic region). The creep data were converted into oscillatory data with the help of NLREG program [36] and later, using the Arrhenius dependency, was shifted to the reference temperature.

C. High-temperature size exclusion chromatography

The MW and MWD characterization was performed by a high-temperature size exclusion chromatograph (HT-SEC 220, Agilent) equipped with three PLGel Olexis columns and with a differential refractive index (RI) detector. The calibration was carried out using polystyrene (PS) standards. The measurement was conducted at 160 °C with 1,2,4-trichlorobenzene eluent, stabilized with 0.2 wt. % of 2,6-di-*tert*-butyl-(4-methylphenol), at a constant flow rate of 1.0 ml/min.

D. Molecular modeling

van Ruymbeke *et al.*, based on the Milner–McLeish theory, developed the TMA for the calculation of relaxation function $G(t)$ for linear chains. The implemented different relaxation mechanisms, such as reptation, contour length fluctuation, and constraint release, allow one to successfully describe the polydisperse samples LVE [34,37,38].

In order to properly take into account the fast and slow relaxation processes, the model describes the relaxation modulus, $G(t)$, as

$$G(t) = G_R(t) + G_d(t), \tag{2}$$

where $G_R(t)$ is responsible for short relaxation processes, i.e., high frequency Rouse processes and longitudinal Rouse modes [34]. The Rouse contribution is related to its MWD through the following linear mixing rule [39,40]:

$$G_R(t) = G_N^0 \left(\int_{-\infty}^{\infty} F_{Rouse}(t, M) w(M) d \log M \right), \tag{3}$$

where G_N^0 is the plateau modulus, $F_{Rouse}(t,M)$ is the Rouse relaxation function of a polymer chain with molecular weight M, and $w(M)$ is the MWD, $dw/dlogM$ in our case [37]. For the investigated multimodal samples, $w(M) = \sum_{i=1}^{4} x_i w_i(M)$, where x_i is the weight fraction of the ith mode of MWD, w_i. Each mode is a log-normal distribution characterized by its width, σ_i, and its position on molar mass axis, M_{c_i}.

On the other hand, $G_d(t)$ corresponds to relaxation processes taking place at time longer than the entanglement relaxation time (τ_e). Including the influence of the constraint release process, it can be defined as

$$G_d(t) = G_N^0 \, \phi(t) \Phi_{tube}(t)^{\alpha}, \tag{4}$$

where $\phi(t)$ represents the polymer fraction not yet relaxed by reptation or fluctuations at time:

$$\phi(t) = \int_{\log M_e}^{\infty} \phi(M, w(M), t) w(M) d \log M, \tag{5}$$

with M_e being the molecular weight between two entanglements and $\phi(M,w(M),t)$ being the survival probability of the polymer chains at time t if the chains have a molecular weight M and are relaxing in a molecular environment $(M,w(M))$. The dilation factor $\Phi_{tube}(t)$ takes into account the fact that the molecular segments relaxed at time t act as a solvent for the remaining unrelaxed chain segments. It is usually equal to $\phi(t)$. The dilution exponent α has been fixed to 1, in agreement with previous works [34,41–45].

To calculate G^* data out of $G(t)$, the Schwarzl approximation was implemented [46]. Furthermore, in order to determine the MWD, in this work we used the "direct problem" approach. To this end, the four-mode log-normal MWD is applied and the discrepancy between the predicted and measured G^*-data is minimized. As a result, we determined x_i, σ_i, and M_{c_i} of all four modes.

III. RESULTS AND DISCUSSION

A. Molecular data

In this study, we prepared by melt blending several PE blends. The polymer matrix was always the same commercially available HDPE but besides varying the reactor blend content we also varied the type of the reactor blend, namely, a RB with 40 wt. % (RB40) and 50 wt. % (RB50) of UHMWPE, respectively. Thus, the obtained trimodal PE blends contain up to 25 wt. % of UHMWPE. The results of molecular weight characterization by HT-SEC of these blends are listed in Tables I and II. Scrutinizing the

TABLE I. Molecular weights and zero-shear viscosity data of the analyzed polymers with RB40 content.

	From HT-SEC			From melt rheology			
Sample	M_w (kg/mol)	$Đ$	M_z/M_w	M_w (kg/mol)	$Đ$	M_z/M_w	η_0[a] (kPa s)
HDPE	75	5.4	4.4	80	4.0	4.0	2.4
5RB40	129	20.5	19.8	105	9.3	11.1	10.6
7.5RB40	139	14.2	16.5	127	11.4	18.6	49.6
10RB40	203	28.2	16.7	240	22.5	32.9	949.7
12.5RB40	214	33.0	14.3	310	30.8	40.6	2 431.4
15RB40	248	40.1	11.3	497	91.3	30.7	8 340.9
20RB40	290	61.0	10.2	943	154	26.5	49 002
30RB40	480	137	7.6	1530	385	14.9	137 227
50RB40	1198	516	2.9	3760[b]	1600[b]	7.7[b]	1.55×10^{6}[c]
100RB40	1092	970	2.9	9000[b,d]	4570[b]	3.4[b]	8.16×10^{6}[c]

[a]Zero-shear viscosity determined experimentally.
[b]Estimated molecular weight values determined by modeling from incomplete LVE data.
[c]Estimated zero-shear viscosity, from fitting the incomplete terminal region using the modified Carreau–Yasuda equation.
[d]In the supplementary material [72], an alternative approach is discussed, which deals with the determination of the MWD and M_w of 100RB40 based on the analysis of blends containing it up to 30 wt. %.

TABLE II. Molecular weights and zero-shear viscosity data of the analyzed polymers with RB50 content. n.d., not determined.

	From HT-SEC			From melt rheology			
Sample	M_w (kg/mol)	$Đ$	M_z/M_w	M_w (kg/mol)	$Đ$	M_z/M_w	η_0[a] (kPa s)
5RB50	117	13.7	8.7	112	10.6	12.6	16.3
7.5RB50	112	13.6	7.8	175	15.4	34.6	293.8
10RB50	202	33.2	9.1	254	22.4	38.7	1 298.6
12.5RB50	154	20.3	12.4	406	35.3	32.7	5 214.6
15RB50	156	27.8	10.1	475	50.5	29.0	7 521.1
17.5RB50	227	37.1	7.4	581	57	26.5	10 426.1
20RB50	292	92.5	12.7	918	117	16.5	37 539.8
30RB50	646	111	6.5	1895	228	13.5	216 537
50RB50	1070	419	4.3	n.d.	n.d.	n.d.	10^{6}[b]
100RB50	1460	1110	2.6	n.d.	n.d.	n.d.	1.4×10^{8}[b]

[a]Zero-shear viscosity determined experimentally.
[b]Estimated zero-shear viscosity, from fitting the incomplete terminal region using the modified Carreau–Yasuda equation.

delivered information, it can be stated that according to HT-SEC analyses, PE blends possess extremely high $Đ$ (up to 1000). Several researchers dealt with unveiling the influence of $Đ$ and M_z/M_w on the rheological behavior of linear PE having a $Đ$ only up to 42 and with an M_z/M_w ratio up to 28, which are significantly lower compared to the here investigated polydispersity levels [19,25,27,47].

The MWD of the studied polymers is shown in Fig. 1. This truly reflects not only the presence of significantly high amount of UHMWPE in the reactor blend but also the multimodality (i.e., multimodal distribution) of the prepared PE blend. Other HT-SEC traces of the RB40 and RB50 series are shown in the supplementary material [72].

The presence of significantly increased weight per cent of UHMWPE in the PE blends may affect blend homogeneity. Investigations showed that RB grants uniformly distributed UHMWPE within HDPE or HDPE/HDPE wax [2,12,13,49–53]. Furthermore, Hofmann *et al.* [14] and Zhong *et al.* [15] recently investigated the thermal properties of a benchmark PE, melt blended from HDPE, HDPE wax, and UHMWPE, via differential scanning calorimetry (DSC). They found that the first heating curve shows, beside the expected melting peak, a second peak at lower temperatures, suggesting phase separation [14,15,49]. The heating curves of PE blends composed of HDPE and bimodal RBs did not exhibit this low temperature peak. Hence, their results further strengthen the earlier published observations of homogeneous trimodal PE blends [12,13,51,52].

B. Thermorheological properties of multimodal PE blends

The rheological behavior of polymer matrix, reactor blend, and multimodal PE blends was investigated by oscillatory and creep measurements. The isotherms gathered from dynamical analysis together with an isotherm recovered from creep measurements are shown in Fig. 2 for some RB40 samples. Plotting phase angle (δ) against the absolute value of the complex modulus ($|G^*|$), the so-called Booij-Palmen plot (BPP), among others, allows us to assess the "modality" [how many well separated relaxation processes can be detected and how they are related to the well separated molecular weights (molecular weight modes, MWMs), see later] and the "shiftability" of isotherms of the samples under investigation.

Discussing "shiftability" we see in Fig. 2 that all HDPE isotherms (square symbols) superimpose, showing a perfect overlap. For multimodal PE blends, the same behavior can be observed. The found degree of overlap proves the thermorheological simplicity of the samples analyzed here. This means that during the measurements no change regarding molecular structure takes place. In addition, by employing the time-temperature superposition (tTS) principle, in order to build master curves, horizontal shifting (a_T) must be

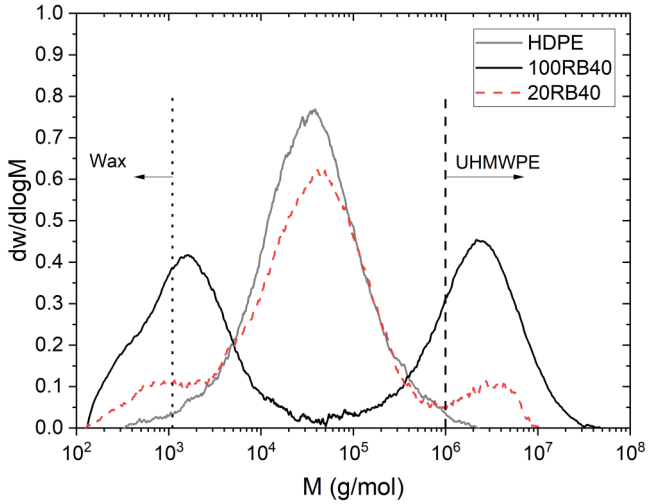

FIG. 1. The HT-SEC trace of HDPE (solid gray line) compared to the pure 100RB40 (solid black line) and 20RB40 (dashed line) of linear PE. The dotted line corresponds to the M_e (1100 g/mol) [48] and the shorter molecules are considered as wax, while the vertical dashed line represents the M_w equal to 10^6 g/mol.

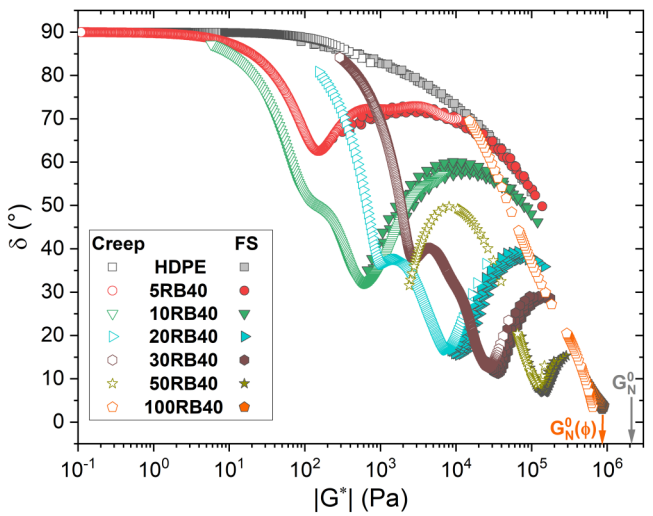

FIG. 2. Phase angle δ versus complex modulus $|G^*|$ for neat HDPE and some PE blends of RB40 series. Full symbols represent the isotherms from dynamical analyses, and the open symbols are calculated with NLREG from creep measurements.

applied only. The usage of vertical shift (b_T) is not necessary [18,54,55].

The analysis of the shift factors a_T in dependence on temperature T allows the determination of flow activation energy (E_a) with the increasing RB40 and RB50 contents, respectively. The resulting E_a values are shown in dependence on UHMWPE content in Fig. 3. The E_a values of the matrix polymer and all trimodal PE blends range between 24 and 33 kJ/mol and are in very good agreement with the literature values. A generally accepted E_a value for the linear PE is 25 kJ/mol [56]. Nevertheless, the literature reports for linear PE values in the range between 20 and 38 kJ/mol [57–61]. The neat RBs (100RB40 and 100RB50) go beyond this limit. Their flow activation energy is slightly higher compared to the reported values. A possible explanation of the increase of flow activation energy might be attributed either to the presence of short- and/or long-chain branching (SCB, LCB) or to the ultrahigh $Đ$ values. Hatzikiriakos investigated the influence of LCB on the rheological properties of PE. They found that LCB content significantly increases the flow activation energy up to 88 kJ/mol compared to 25 kJ/mol (linear PE) [18]. In contrast, the PE samples, analyzed by Wasserman and Graessley, with potential LCB content do not corroborate the elevation of flow activation energy [62]. Moreover, applying tTS principle in order to obtain master curves of the samples with LCB content, besides horizontal shift a vertical shift was also necessary in their case [18,54,55]. Stadler *et al.* analyzed the effects of SCB of PE on the E_a. They came to the conclusion that the presence of significant concentration of SCB (more than 20 wt. %) leads to the increase of E_a [60]. However, such a high SCB content is impossible for our samples due to synthesis conditions.

The effect of polydispersity on activation energy must be analyzed as well. Hatzikiriakos observed that the influence of high $Đ$ has similar effects as the presence of LCB, i.e., both of them lead to the increased E_a [18]. Some of linear HDPE investigated by Ansari *et al.* showed increased E_a as well, and they attributed the increase of E_a to the high polydispersity [19].

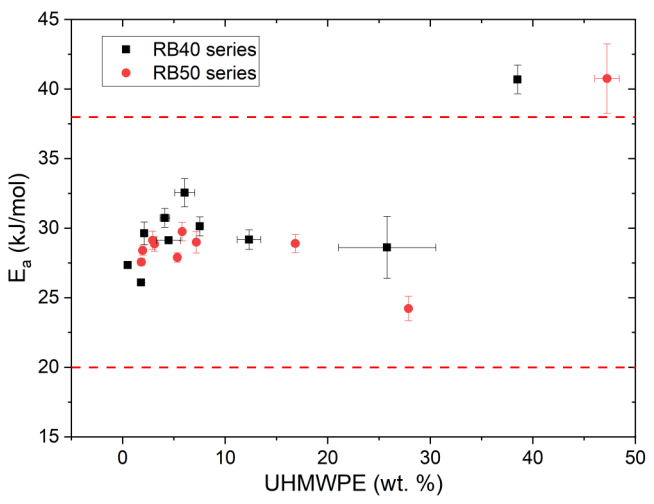

FIG. 3. The change of flow activation energy of polymer matrix (HDPE) with increasing UHMWPE content.

The here studied trimodal PE blends and RBs are characterized by thermorheological simplicity, and master curves are obtained by horizontal shifting only. Therefore, it seems that in the present case the high E_a values of RBs are attributed to the extremely high $Đ$ rather than to the presence of potential LCB. However, due to the lack of a triple detector HT-SEC (refractive index, viscometer, and light scattering), we cannot completely exclude the possibility of very few branched chains, because of the used catalysts for which chain walking mechanism can result in LCB [63].

Now, we are analyzing how the appearance of the samples minima in BPP is influenced by their modality of MWD (Fig. 2). Starting with monomodal HDPE at low $|G^*|$, the curve shows a plateau at $\delta = 90°$ representing the terminal relaxation region of this polymer. With increasing $|G^*|$, the course of δ is continuously decreasing, without reaching the minimum at ~2.1 MPa, which is the G_N^0 of linear PE [64–66]. In the modulus range $|G^*| < G_N^0$, no local minima can be detected that is in agreement with the monomodal character of MWD (no wax, no UHMWPE). Switching to 100RB40, in the expected G_N^0 range, a minimum can be seen at ~0.85 MPa, a value which is shifted to lower values compared to the known 2.1 MPa. HT-SEC measurements revealed that 100RB40 contains of about 37 wt. % wax, which acts as a solvent for longer chains. The plateau modulus of a diluted entanglement network, $G_N^0(\varphi)$, can be calculated according to [67]

$$G_N^0(\varphi) = G_N^0 \cdot \varphi^2, \tag{6}$$

where φ is the weight fraction of polymer chains with $M_w > M_e$. The calculated value of about 0.83 MPa is in good agreement with the experiment. In modulus range $|G^*(\omega)| < G_N^0(\varphi)$, no additional minimum can be found. This is in agreement with HT-SEC because the mode around M_e must be considered as solvent not leading to an additional local minimum in BPP.

Multimodal PE blends show different behavior compared to the neat HDPE or RB40. For example, 20RB40 is characterized by two well separated minima at $|G^*| = 10^3$ and 10^4 Pa, respectively. Furthermore, it can be observed that the minimum at high $|G^*|$ values, which corresponds to the "diluted" plateau modulus $G_{N_{20RB40}}^0(\varphi)$, is missing due to the PE-specific limitations in an accessible frequency range. However, due to the fact that 20RB40 contains less wax compared to 100RB40 but more than the HDPE, the $G_{N_{20RB40}}^0(\varphi)$ is expected between the neat PEs G_N^0 and 100B40s $G_N^0(\varphi)$. It is noteworthy to mention that all multimodal PE blends, similar to 20RB40, are characterized by two minima in the modulus range $|G^*| < G_N^0$, which are more or less pronounced.

Trinkle and Friedrich analyzed how distinct relaxation processes of a polymer influence the shape of the BPP [64,68]. In particular, they found that bimodality of a polymer blend (a mixture of linear chains of two lengths) causes two minima separated by a local maximum. The first minimum at high $|G^*|$ corresponds to G_N^0, and the second minimum at smaller $|G^*|$ is related to the relaxation of species with the higher molecular weight. It should be emphasized that if one MWM of the multimodal MWD is characterized by $M_w < M_e$, its

effect will be seen as G_N^0-shift according to Eq. (6) only and it will not lead to the appearance of additional minimum in the modulus range $|G^*|<G_N^0$. Accordingly, the trimodal PE blends should result in a bimodal BPP with a shift of the plateau modulus to lower values due to dilution by waxy PE. Thus, based on HT-SEC measurements, we should expect the appearance of two minima in BPP, a first one at $G_N^0(\varphi)$ and another one in the modulus range $|G^*| < G_N^0(\varphi)$. This is in conflict with experimental data highlighted in BPP, which, in case of all multimodal PE blends, show in total three minima, two of that are in the modulus range $|G^*| < G_N^0(\varphi)$. This suggests that the third minimum (with higher δ value) corresponds to an additional UHMWPE contribution, certainly beyond the exclusion limit of the SEC setup. Consequently, we expect that a rheologically determined MWD of multimodal PE blends will contain not two but three well separated molar weight modes besides the low molecular weight (wax) mode. Therefore, in the determination of the MWD from rheology, we should account for the possibility that multimodal PE blends are characterized by tetramodal rather than a trimodal MWD. Furthermore, it must be noted that the appearance of the local minima in the BPP plot is another hint on the homogeneity of all samples. The full set of BPP, loss-, and storage modulus data of this series together with all samples of the RB50 series is given in the supplementary material [72].

C. η_0 scaling relation

Based on these master curves, we can now analyze the terminal relaxation behavior in terms of zero-shear viscosity. The change of the η_0 (details regarding η_0 determination can be found in the supplementary material [72]) versus M_w determined by HT-SEC is presented in Fig. 4. In addition, besides our multimodal PE blends, several mono- and polydisperse PE data taken from the literature [25,27,47] are included and compared with our data (Fig. 4). It can be seen

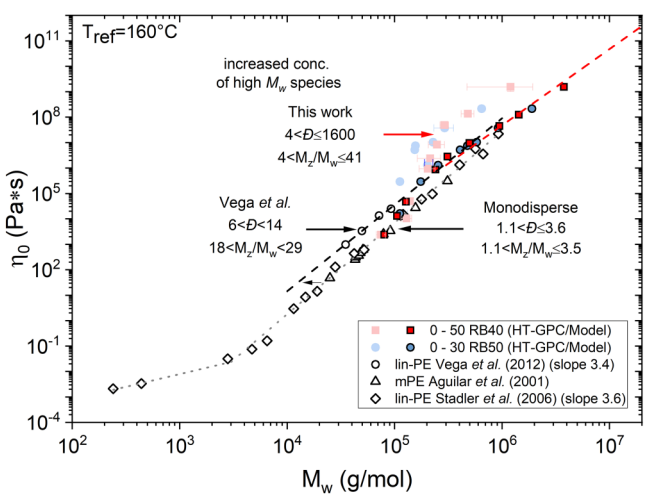

FIG. 4. Zero-shear viscosity η_0 versus weight average molecular weight M_w in the double logarithmic plot for PE blends (experimental data and modeling) and literature data. The pale square and pale circle full symbols represent the zero-shear viscosity of all PE blends with RB40 and RB50 as a function of M_w obtained from HT-SEC measurements. The filled square and circle symbols with black edges represent the viscosities versus corrected M_w obtained from modeling. The red dashed line has a slope of 3 and is the linear fit of the here analyzed multimodal samples with $M_w > 700$ kg/mol.

that the viscosities of polymer matrix (HDPE) and trimodal PE blends up to M_w of about 120 kg/mol (2.5 wt. % of UHMWPE) follow the known scaling relation of monodisperse or slightly polydisperse PE samples (with $Đ$ up to 4). With increasing M_w and $Đ$, the zero-shear viscosity, compared to the monodisperse samples, shifts to higher values (see the pale symbols), approaching and going beyond the line proposed by Vega *et al.*, who investigated the influence of MWD and high molecular weight species on the zero-shear viscosity of PE [27]. They found that polydisperse PE samples with increased M_z/M_w ratio (between 18 and 29) show higher η_0 compared to monodisperse ones, but still follow the scaling relation, showing a slope of 3.4. Thus, these shifts to higher η_0 values of trimodal PE blends can be attributed to the increased $Đ$ (~30, according to HT-SEC) and M_z/M_w ratio (~17, according to HT-SEC). A further increase of the UHMWPE content above 5 wt. % corresponding to $M_w = 200$ kg/mol leads to an extraordinary increase of η_0. A significant discrepancy between viscosity predicted by scaling relations of either monodisperse or polydisperse (Vega line) samples and those of multimodal PE blends can be observed. We attribute this deviation to incorrectly determined molecular weights, which seem to be underestimated. Earlier, analyzing the E_a, we came to the conclusion that the effect of very few LCB on LVE, if there are any, is negligible. Furthermore, the analysis of the BPP suggested the existence of an additional UHMWPE mode, which would raise the characteristic molecular weights significantly.

Therefore, we analyze the LVE data of all blends in relation to a "rheological" (in contrast to HT-SEC) MWD, which is in agreement with these data.

D. MWD determination by modeling

With the help of TMA, we first predicted the LVE of multimodal PE blends from its MWD (determined by HT-SEC) and compared with the given G^* data (see Fig. 5). At high frequencies, above 1 rad/s a good agreement between experimentally given and calculated moduli can be observed. However, at lower frequencies, which correspond to longer relaxation times and higher molar masses, systematic deviation is observed. While the discrepancy is important, it corresponds to a low fraction of chains, of around $\sqrt{10^2/G_N^0} = 0.7$ wt. % of the sample. Hence, we attribute the differences between the predicted and measured curves to the lack of long chains with molecular weights in the UHMW region. This is the region, which is mostly influenced by experimental problems with HT-SEC [29,31].

In order to bring the MWD of multimodal PE blends in agreement with LVE measurements, we had to significantly modify the high molecular weight tail of that polymer by adding a fourth mode, expected from the analysis of BPP (see Fig. 6). Now, using tetramodal distribution the predicted and experimental master curves are in very good agreement (Fig. 5). In the modeled MWD, this additional mode only represents 0.7 wt. % of the total sample.

The aforementioned method was applied to all multimodal PE blends containing RB40 and RB50. The characteristic

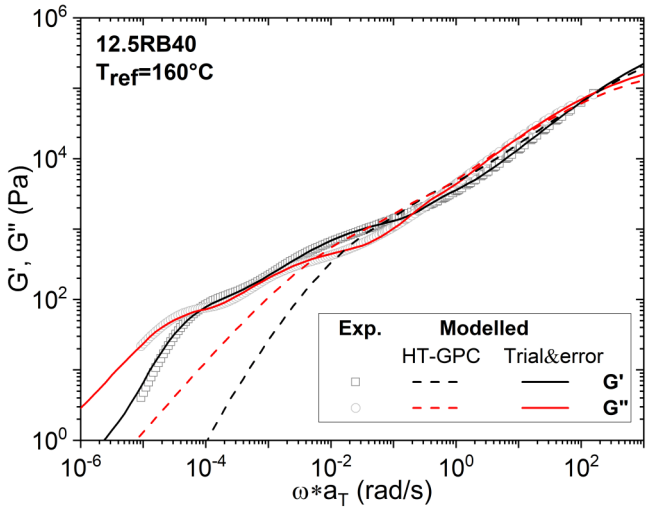

FIG. 5. Storage G' and loss G'' moduli versus frequency ωa_T in the double logarithmic plot. Open symbols represent the experimental data; dashed lines show the predicted master curve according to MWD determined by HT-SEC; solid lines represent simulation. The model based on the TMA successfully describes multimodal PE blends.

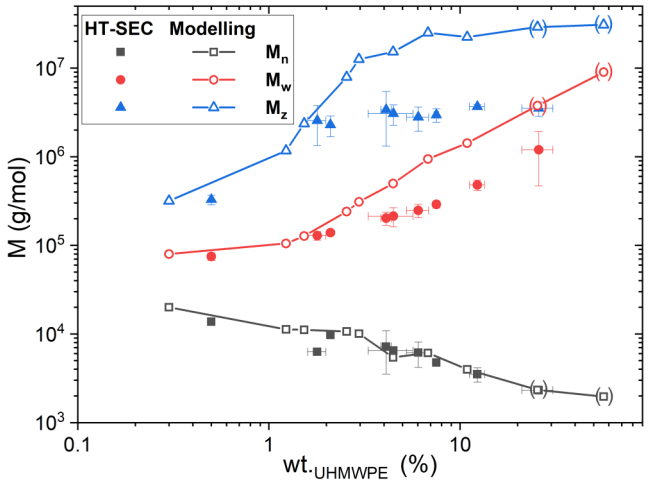

FIG. 7. Characteristic molecular weights determined by HT-SEC and modeling versus the UHMWPE content for RB40 series. The brackets symbolize that the terminal regions for 50RB40 and 100RB40 were not completely uncovered and the real molecular weight may deviate from the presented one. The characteristic molecular weight data (below 0.7 wt. %) correspond to the neat HDPE, determined by HT-SEC and Modeling.

molecular weights determined by modeling are shown in Tables I and II. The experimental moduli and those obtained from modeling superimpose very well and the corresponding figures are presented in the supplementary material [72]. However, we have to admit that this superior agreement was only possible by fitting the MWD of the two UHMW modes for every blend individually. The resulting modeling parameters such as weight fractions of each mode and the corresponding characteristic molecular weights are given in the supplementary material [72]. Analyzing the MWD obtained by modeling (see the supplementary material [72]), it can be stated that the increase of RB40 or RB50 content leads to a systematic increase of the fourth mode. The information received from rheological analysis and modeling showed that HT-SEC fails to properly determine the MWD of multimodal PE blends with ultra-broad distribution and with extraordinarily long chain ($M_w > 10^7$ g/mol) content. Furthermore, we successfully validated TMA which properly predicts the

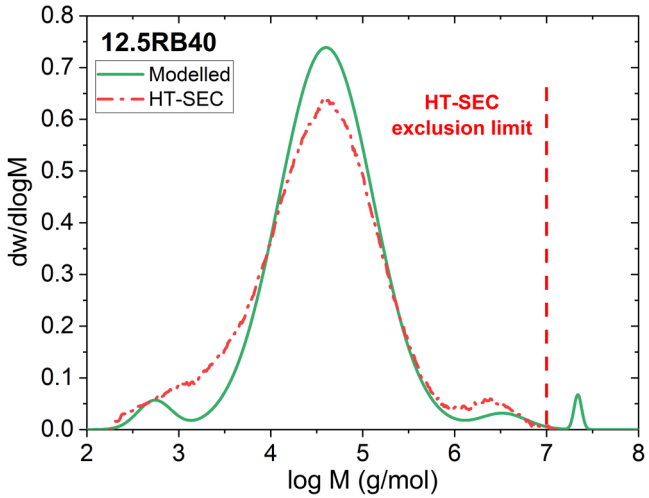

FIG. 6. MWD obtained from HT-SEC measurement and modeling.

molecular dynamics of ultra-broad molecular weight distributed ($Đ \approx 1000$) linear entangled PE.

Comparing the characteristic molecular weights determined via HT-SEC and modeling (see Fig. 7), it can be stated that no significant differences between the M_n values can be observed for all samples. However, if other characteristic molecular weights M_w and M_z are analyzed, where the proper estimation of long chains is crucial, notable discrepancy between the values determined either by HT-SEC or modeling can be seen starting from 2 wt. % of UHMWPE content. These differences may be attributed to those HT-SEC drawbacks, which were discussed by Suzuki *et al.* and Mes *et al.* [29,31].

E. Correction scheme for polydispersity

The η_0 of multimodal PE blends versus their M_w determined with the TMA model are presented in Fig. 4 as well (see filled symbols). It can be observed that now all viscosities lie in the region of the two straight lines for mono- and polydisperse PE. Only the viscosities of the samples with the highest molecular weight and highest polydispersity seem to fall under the line for monodisperse samples. For those PE, the transition to the pure reptation regime can be expected because their M_w is larger than the given M_r.

Obviously, unveiling the real M_w of the ultra-broad MWD PE blends gives access to analyze the transitional zone where $\eta_0 \propto M_w^{3.4}$ and M_w^3. The zero-shear viscosity starts to scale with M_w^3 when the M_w is higher than the reptation molecular weight M_r. To determine M_r, first of all a correction on the Newtonian viscosity should be applied which takes into account the polydispersity effect of the PE blends. Therefore, we analyze the influence of characteristic molecular weights on η_0, by plotting $\eta_0$versus the characteristic molecular weights, M_n, M_w, and M_z, respectively (see top of Fig. 8). For monodisperse PE samples, independently of the choice of characteristic molecular weight, a similar trend is

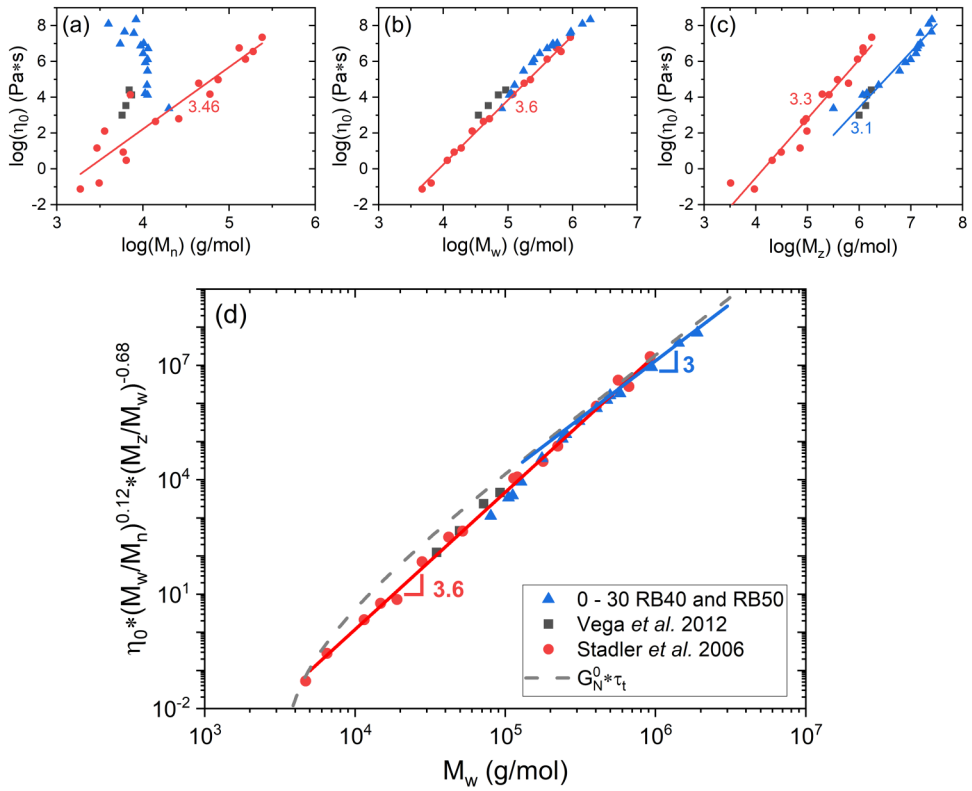

FIG. 8. Zero-shear viscosity versus weight average molecular weight for different PE in a double logarithmic plot at a reference temperature $T_{ref} = 160\,°C$; (a) is $\log(\eta_0)$ dependence on the $\log(M_n)$; (b) is $\log(\eta_0)$ dependence on the $\log(M_w)$; (c) is $\log(\eta_0)$ dependence on the $\log(M_z)$, and (d) is the scaling relation of the normalized η_0 as a function of M_w.

observed, leading to a power law with a slope between 3.3 and 3.6. However, analyzing $\eta_0$versus M_n and M_z for broad and ultra-broad distributed PE, significant differences compared to the monodisperse samples can be seen. The viscosity scaling is almost identical to those of narrow distributed samples if M_w is used as characteristic molecular weight, although with an offset to higher η_0 values [see Fig. 8(b)]. Moreover, all data presented in Fig. 8(b) reveal that the power law exponent is 3.6 rather than 3.4. Exponents reported in the literature lay between 3.4 [21,27] and 3.6 [25,62]. Our analysis confirms the higher value, 3.6.

Now, we are looking for an appropriate scheme, which allows to properly take into account the polydispersity. While for monodisperse samples the scaling relation between zero-shear viscosity (η_0) versus molecular weight is well known, it is yet to be determined for polydisperse samples, especially those with ultra-broad MWD.

We use the following scaling relation as a starting point for the analysis:

$$\eta_0 = K \cdot M_n^a \cdot M_w^b \cdot M_z^c \cdot M_{z+1}^d \cdot M_{z+2}^e \cdot \cdots, \tag{7}$$

where K is a material parameter, M_z is the z-average molecular weight, M_{z+1} is the $(z+1)$-average molecular weight, and so on. Furthermore, a, b, c, d, e, … are the power law exponents of the characteristic molecular weights. We restrict our analysis to the values of a, b, c, only and assume $d = e = \cdots = 0$, because the determination of higher moments is becoming prone to increasing errors. In order to fit our data, we transformed Eq. (7) into the following form:

$$\log(\eta_0) = k + a \cdot x_n + b \cdot x_w + c \cdot x_z, \tag{8}$$

where k [equal to $\log(K)$] is a constant and $x_i = \log(M_i)$, $i = n,\ m,\ z$. Moreover, we restrict our data analysis to the M-range below 700 kg/mol. We chose this upper limit because according to the literature the reptation molecular weight is $M_{r_{lit.}} \approx 800\,\mathrm{kg/mol}$ [21,23]. Therefore, for higher M, a change in the slope is expected. Furthermore, the fitting itself was performed with a linear hyper-plane fitting algorithm implemented in ORIGINPRO 2019. During the fitting procedure, all parameters were set free and a, b, and c are not subjected to any side conditions. The fitting resulted in $k = -14.332 \pm 0.255$, $a = 0.12 \pm 0.11$, $b = 2.8 \pm 0.18$, and $c = 0.68 \pm 0.087$.

Analyzing the power law exponents (a, b, and c), it can be seen that the sum of them is equal to 3.6. This fact strengthens the assumption that η_0 versus characteristic molecular weight scales with 3.6 rather than with 3.4.

Applying the parameters together with Eq. (8) and assuming that M_w is the most relevant characteristic molecular weight for scaling relation, the result can be transformed and yields the following equation:

$$\eta_0 = \mathrm{K} \cdot M_n^{0.12} \cdot M_w^{2.8} \cdot M_z^{0.68} = \mathrm{K} \cdot M_w^{\alpha} \cdot \left(\frac{M_w}{M_n}\right)^{\beta} \cdot \left(\frac{M_z}{M_w}\right)^{\gamma}$$
$$= \eta_{0_{mono}} \cdot \left(\frac{M_w}{M_n}\right)^{\beta} \cdot \left(\frac{M_z}{M_w}\right)^{\gamma}, \tag{9}$$

where K is a prefactor, $\alpha = 3.6$, $\beta = -0.12$, and $\gamma = 0.68$. Thus, the influence of polydispersity on zero-shear viscosity can be accounted for by calculating a corrected $\eta_{0_{corr}}$,

$$\eta_{0_{corr}} = \eta_{0_{mono}} = \eta_0 \cdot \left(\frac{M_w}{M_n}\right)^{0.12} \cdot \left(\frac{M_z}{M_w}\right)^{-0.68} \propto M_w^{3.6}. \quad (10)$$

According to this equation, the corrected viscosity of a sample of any MWD corresponds to the viscosity of a monodisperse sample having the same M_w as the polydisperse sample. We can then apply this scheme to all the data including those samples which are expected to have $M_w > M_r$ and analyze the viscosities of all the samples. As shown in Fig. 8(d), plotted in such a way, the viscosities are well independent of the form of their individual MWDs. Data shown in Fig. 8(d) are taken as the basis for the analysis in Sec. III F.

It must be noted that Wasserman and Graessley [62] proposed a similar correction and found that the M_z/M_w ratio is the most important. Their scaling relation coincides with Eq. (9) with $\alpha = 3.6$, $\beta = 0$, and $\gamma = 1$. The differences between their and the here found correlation are illustrated in the supplementary material [72]. They found that this correlation can be applied not only for PE but also for polypropylene (PP). The polydispersity effect, taking into account the influence of M_n, M_w, M_z on the LVE of entangled polymers, was keenly investigated by Nobile and Cocchini [69] as well. Their analyses, including PE with $M_w/M_n < 6$ and $M_z/M_w < 3$, proposed that the ratios of characteristic molecular weights, $(M_w/M_n)^{0.19} \cdot (M_z/M_w)^{0.4}$, had to be used in order to determine the zero-shear viscosity. Later, they simplified this expression by neglecting the influence of M_w/M_n and found that $\eta_0 \propto 0.51 \cdot M_w^{3.4} \cdot (M_z/M_w)^{0.8}$ is the best representation of their data (see the supplementary material [72]). Vega *et al.* confirmed Nobile's proposal for linear PE with a $Đ$ up to 14 and an M_z/M_w ratio up to 28 [27]. However, our analysis shows that the influence of extremely high polydispersity can be properly accounted for if Eq. (10) is applied.

Since from Eq. (10), one can determine the molar mass of the monodisperse sample having a viscosity equivalent to the observed polydisperse sample, we can also determine the terminal relaxation time, τ_t, from the zero-shear viscosity, assuming that the sample is monodisperse (thus $\eta_0 = G_N^0 \cdot \tau_t$), and compare this value with the prediction obtained with tube-models proposed in the literature. The τ_t was determined by reptation model which takes into account the contour length fluctuation [33,70]:

$$\tau_t = 3\tau_e \left(\frac{M_w}{M_e}\right)^3 \left[1 - \kappa \left(\frac{M_w}{M_e}\right)^{-0.5}\right]^2, \quad (11)$$

where $\kappa = 1.69$ [71], $\tau_e = 4.4$ ns [48], and $M_e = 1100$ g/mol [48]. The comparison (see Fig. 8) shows very good agreement between experimental and predicted data, especially in the pure reptation region, and thus strengthens the pertinence of our analysis.

F. Reptation molecular weight

Due to the fact that some of our multimodal PE blends have molecular weights significantly larger than the so far given reptation molecular weight M_r, we are able to determine this value experimentally.

To this end, we analyze the scaling behavior of those samples, which have M_w values larger than 700 kg/mol. These data are given in Fig. 8 and follow a linear dependency with a slope of 3 (see line in Fig. 8). The characteristic molecular weight M_r is the crossover molecular weight defined by the crossover of the two straight lines with a slope of 3.6 and 3, respectively. Details of this analysis can be found in the supplementary material [72]. However, we have to admit that the applied procedure is not fully "objective," because the used molecular dynamics model contains implicitly the transition in the viscosity scaling from an exponent of ~3.5 to an exponent of 3.0. This is a property of the model in agreement with experimental facts and a prerequisite for the correct determination of MWD. Insofar, the predicted molar mass distributions, and therefore, the characteristic molecular weights such as M_w and M_r, are influenced by the model. Our analysis led to $M_r = 560^{+150}_{-118}$ kg/mol. Reported data range between 620 and 800 kg/mol [21,23]. Our determined value is slightly below the reported data. However, it must be noted that Vega *et al.* determined M_r by analyzing the transition zone between the regions with slopes 3.4 and 3. Due to the fact that their power law exponent is smaller compared to 3.6, the crossover point for PE shifts to the higher values (~220 M_c), thus leading to the increased M_r value (in comparison to the here presented value).

IV. CONCLUSIONS

In this work, we have investigated the linear viscoelastic properties of multimodal PE blends of linear chains, containing a significant amount of UHMWPE (up to 50 wt. %) and therefore having ultrahigh polydispersity. The analysis of the LVE data using BPPs confirmed Trinkle's finding [64] that multimodal blends besides the plateau modulus' minimum show other minima which are attributed to well separated relaxation regions, and which we could associate with well separated MWMs.

The determined flow activation energy unveils that all multimodal PE blends are characterized by E_a values similar to that of the polymer matrix (~27 kJ/mol). However, E_a values of neat RBs are increased (~41 kJ/mol). This is attributed to the ultra-broad MWD rather than to the presence of very few LCB.

Moreover, samples with ultrahigh $Đ$ and notably increased M_z/M_w ratio cause a significant contribution to the zero-shear viscosity, leading to significantly higher η_0 values compared to monodisperse and polydisperse samples known so far. This discrepancy was attributed to the incorrectly determined (underestimated) M_w from HT-SEC measurements. To overcome these problems, the linear viscoelastic data were analyzed with an appropriate molecular dynamics model, namely, with TMA, yielding the "rheological" MWD and, consequently, the corresponding characteristic molecular weights (M_n, M_w, and M_z). Until now, the TMA model was validated for mono- and

moderately polydisperse samples only. The very good agreement between experimentally obtained and calculated viscosities lets us to conclude that the model is successfully applicable for ultra-broad molecular weight distributed linear PE blends as well.

Investigating the polydispersity effects on η_0, it was found that these can be taken into account if η_0 is corrected with the factor $(M_w/M_n)^{0.12}(M_z/M_w)^{-0.68}$. The analysis of the viscosities corrected in this way and plotted as a function of M_w below the reptation molecular weight revealed a power law dependence with a slope of 3.6 rather than 3.4. Finally, the analysis of all viscosities including those from the samples with the highest M_w led to the determination of the reptation molecular weight of linear PE, which amounts to 560^{+150}_{-118} kg/mol.

ACKNOWLEDGMENTS

L.Sz., Y.F., F.Z., T.H., R.M., and C.F. are grateful to BMBF for financial support within the CATEFF project. L.Sz. thanks Dr. B. Mélykúti for the valuable discussions. E.V.R. is chercheur qualifie of the Fonds National de la Recherche Scientifique (FNRS).

REFERENCES

[1] Spalding, M. A., and A. M. Chatterjee, *Handbook of Industrial Polyethylene and Technology* (John Wiley & Sons, Hoboken, NJ, 2017).

[2] Stürzel, M., S. Mihan, and R. Mulhaupt, "From multisite polymerization catalysis to sustainable materials and all-polyolefin composites," Chem. Rev. **116**, 1398–1433 (2016).

[3] Plastics Pipe Institute, *Handbook of Polyethylene Pipe* (The Plastics Pipe Institute, Irving, TX, 2008).

[4] Allal, A., A. Lavernhe, B. Vergnes, and G. Marin, "Relationships between molecular structure and sharkskin defect for linear polymers," J. Nonnewton. Fluid Mech. **134**, 127–135 (2006).

[5] Jugo Viloria, M., M. Valtier, and B. Vergnes, "Volume instabilities in capillary flow of pure SBR and SBR compounds," J. Rheol. **61**, 1085–1097 (2017).

[6] Denn, M. M., "Extrusion instabilities and wall slip," Annu. Rev. Fluid Mech. **33**, 265–287 (2001).

[7] Marichin, V. A., L. P. Mjasnikova, D. Zenke, R. Hirte, and P. Weigel, "Ultra-high strength and ultra-high modulus fibers from polyethylene," Polym. Bull. **12**, 287–292 (1984).

[8] Lafleur, S., R. Berthoud, R. Ensinck, A. Cordier, G. de Cremer, A. Philippaerts, K. Bastiaansen, T. Margossian, and J. R. Severn, "Tailored bimodal ultra-high molecular weight polyethylene particles," J. Polym. Sci. Part A Polym. Chem. **56**, 1645–1656 (2018).

[9] Kelly, J. M., "Ultra-high molecular weight polyethylene," J. Macromol. Sci. Polym. Rev. **42**, 355–371 (2002).

[10] Boscoletto, A. B., R. Franco, M. Scapin, and M. Tavan, "An investigation on rheological and impact behaviour of high density and ultra high molecular weight polyethylene mixtures," Eur. Polym. J. **33**, 97–105 (1997).

[11] Aguilar, M., S. Martín, J. F. Vega, A. Muñoz-Escalona, and J. Martínez-Salazar, "Processability of a metallocene-catalyzed linear PE improved by blending with a small amount of UHMWPE," J. Polym. Sci. B Polym. Phys. **43**, 2963–2971 (2005).

[12] Kurek, A., S. Mark, M. Enders, M. O. Kristen, and R. Mülhaupt, "Mesoporous silica supported multiple single-site catalysts and polyethylene reactor blends with tailor-made trimodal and ultra-broad molecular weight distributions," Macromol. Rapid Commun. **31**, 1359–1363 (2010).

[13] Stürzel, M., A. G. Kurek, T. Hees, Y. Thomann, H. Blattmann, and R. Mülhaupt, "Multisite catalyst mediated polymer nanostructure formation and self-reinforced polyethylene reactor blends with improved toughness/stiffness balance," Polymer **102**, 112–118 (2016).

[14] Hofmann, D., A. Kurek, R. Thomann, J. Schwabe, S. Mark, M. Enders, T. Hees, and R. Mülhaupt, "Tailored nanostructured HDPE wax/UHMWPE reactor blends as additives for melt-processable all-polyethylene composites and in situ UHMWPE fiber reinforcement," Macromolecules **50**, 8129–8139 (2017).

[15] Zhong, F., J. Schwabe, D. Hofmann, J. Meier, R. Thomann, M. Enders, and R. Mülhaupt, "All-polyethylene composites reinforced via extended-chain UHMWPE nanostructure formation during melt processing," Polymer **140**, 107–116 (2018).

[16] Hees, T., F. Zhong, C. Koplin, R. Jaeger, and R. Mülhaupt, "Wear resistant all-PE single-component composites via 1D nanostructure formation during melt processing," Polymer **151**, 47–55 (2018).

[17] Dealy, J. M., and R. G. Larson, *Structure and Rheology of Molten Polymers: From Structure to Flow Behavior and Back Again* (Hanser, Munich, 2006).

[18] Hatzikiriakos, S. G., "Long chain branching and polydispersity effects on the rheological properties of polyethylenes," Polym. Eng. Sci. **40**, 2279–2287 (2000).

[19] Ansari, M., S. G. Hatzikiriakos, A. M. Sukhadia, and D. C. Rohlfing, "Rheology of Ziegler–Natta and metallocene high-density polyethylenes: Broad molecular weight distribution effects," Rheol. Acta **50**, 17–27 (2011).

[20] Ferry, J. D., *Viscoelastic Properties of Polymers* (Wiley, New York, 1980).

[21] Vega, J. F., S. Rastogi, G. W. M. Peters, and H. E. H. Meijer, "Rheology and reptation of linear polymers. Ultrahigh molecular weight chain dynamics in the melt," J. Rheol. **48**, 663–678 (2004).

[22] Fetters, L. J., D. J. Lohse, S. T. Milner, and W. W. Graessley, "Packing length influence in linear polymer melts on the entanglement, critical, and reptation molecular weights," Macromolecules **32**, 6847–6851 (1999).

[23] Unidad, H. J., M. A. Goad, A. R. Bras, M. Zamponi, R. Faust, J. Allgaier, W. Pyckhout-Hintzen, A. Wischnewski, D. Richter, and L. J. Fetters, "Consequences of increasing packing length on the dynamics of polymer melts," Macromolecules **48**, 6638–6645 (2015).

[24] Colby, R. H., L. J. Fetters, and W. W. Graessley, "The melt viscosity-molecular weight relationship for linear polymers," Macromolecules **20**, 2226–2237 (1987).

[25] Stadler, F. J., C. Piel, J. Kaschta, S. Rulhoff, W. Kaminsky, and H. Münstedt, "Dependence of the zero shear-rate viscosity and the viscosity function of linear high-density polyethylenes on the mass-average molar mass and polydispersity," Rheol. Acta **45**, 755–764 (2006).

[26] Otegui, J., J. Ramos, J. F. Vega, and J. Martínez-Salazar, "Effect of high molar mass species on linear viscoelastic properties of polyethylene melts," Eur. Polym. J. **49**, 2748–2758 (2013).

[27] Vega, J. F., J. Otegui, J. Ramos, and J. Martínez-Salazar, "Effect of molecular weight distribution on Newtonian viscosity of linear polyethylene," Rheol. Acta **51**, 81–87 (2012).

[28] Wingstrand, S. L., B. Shen, J. A. Kornfield, K. Mortensen, D. Parisi, D. Vlassopoulos, and O. Hassager, "Rheological link between polymer melts with a high molecular weight tail and enhanced formation of Shish-Kebabs," ACS Macro Lett. **6**, 1268–1273 (2017).

[29] Suzuki, N., Y. Masubuchi, Y. Yamaguchi, T. Kase, T. K. Miyamoto, A. Horiuchi, and T. Mise, "Olefin polymerization using highly congested ansa-metallocenes under high pressure: Formation of super-high molecular weight polyolefins," Macromolecules **33**, 754–759 (2000).

[30] Talebi, S., R. Duchateau, S. Rastogi, J. Kaschta, G. W. M. Peters, and P. J. Lemstra, "Molar mass and molecular weight distribution determination of UHMWPE synthesized using a living homogeneous catalyst," Macromolecules **43**, 2780–2788 (2010).

[31] Mes, E. P. C., H. de Jonge, T. Klein, R. R. Welz, and D. T. Gillespie, "Characterization of high molecular weight polyethylenes using high temperature asymmetrical flow field-flow fractionation with on-line infrared, light scattering, and viscometry detection," J. Chromatogr. A **1154**, 319–330 (2007).

[32] Doi, M., and S. F. Edwards, *The Theory of Polymer Dynamics* (Clarendon, Oxford, 1986).

[33] Milner, S. T., and T. C. B. McLeish, "Reptation and contour-length fluctuations in melts of linear polymers," Phys. Rev. Lett. **81**, 725–728 (1998).

[34] van Ruymbeke, E., C.-Y. Liu, and C. Bailly, "Quantitative tube model predictions for the linear viscoelasticity of linear polymers," in *Rheology Reviews 2007*, edited by D. M. Binding, N. E. Hudson, and R. Kevnings (The British Society of Rheology, 2007), pp. 53–134.

[35] Winter, H. H., and M. Mours, "The cyber infrastructure initiative for rheology," Rheol. Acta **45**, 331–338 (2006).

[36] Honerkamp, J., and J. Weese, "A nonlinear regularization method for the calculation of relaxation spectra," Rheol. Acta **32**, 65–73 (1993).

[37] van Ruymbeke, E., R. Keunings, and C. Bailly, "Determination of the molecular weight distribution of entangled linear polymers from linear viscoelasticity data," J. Nonnewton. Fluid Mech. **105**, 153–175 (2002).

[38] van Ruymbeke, E., A. Kaivez, A. Hagenaars, D. Daoust, P. Godard, R. Keunings, and C. Bailly, "Characterization of sparsely long chain branched polycarbonate by a combination of solution, rheology and simulation methods," J. Rheol. **50**, 949–973 (2006).

[39] Tsenoglou, C., "Molecular weight polydispersity effects on the viscoelasticity of entangled linear polymers," Macromolecules **24**, 1762–1767 (1991).

[40] des Cloizeau, J., "Double reptation vs. simple reptation in polymer melts," Europhys Lett. **6**, 475 (1988).

[41] van Ruymbeke, E., Y. Masubuchi, and H. Watanabe, "Effective value of the dynamic dilution exponent in bidisperse linear polymers: From 1 to 4/3," Macromolecules **45**, 2085–2098 (2012).

[42] van Ruymbeke, E., V. Shchetnikava, Y. Matsumiya, and H. Watanabe, "Dynamic dilution effect in binary blends of linear polymers with well-separated molecular weights," Macromolecules **47**, 7653–7665 (2014).

[43] Park, S. J., and R. G. Larson, "Dilution exponent in the dynamic dilution theory for polymer melts," J. Rheol. **47**, 199–211 (2003).

[44] van Ruymbeke, E., R. Keunings, and C. Bailly, "Prediction of linear viscoelastic properties for polydisperse mixtures of entangled star and linear polymers: Modified tube-based model and comparison with experimental results," J. Nonnewton. Fluid Mech. **128**, 7–22 (2005).

[45] Auhl, D., P. Chambon, T. C. B. McLeish, and D. J. Read, "Elongational flow of blends of long and short polymers: Effective stretch relaxation time," Phys. Rev. Lett. **103**, 136001 (2009).

[46] Schwarzl, F. R., "Numerical calculation of storage and loss modulus from stress relaxation data for linear viscoelastic materials," Rheol. Acta **10**, 165–173 (1971).

[47] Aguilar, M., J. F. Vega, E. Sanz, and J. Martínez-Salazar, "New aspects on the rheological behaviour of metallocene catalysed polyethylenes," Polymer **42**, 9713–9721 (2001).

[48] Szántó, L., R. Vogt, J. Meier, D. Auhl, E. van Ruymbeke, and C. Friedrich, "Entanglement relaxation time of polyethylene melts from high-frequency rheometry in the mega-hertz range," J. Rheol. **61**, 1023–1033 (2017).

[49] Stürzel, M., Y. Thomann, M. Enders, and R. Mülhaupt, "Graphene-supported dual-site catalysts for preparing self-reinforcing polyethylene reactor blends containing UHMWPE nanoplatelets and in situ UHMWPE Shish-Kebab nanofibers," Macromolecules **47**, 4979–4986 (2014).

[50] Stürzel, M., T. Hees, M. Enders, Y. Thomann, H. Blattmann, and R. Mülhaupt, "Nanostructured polyethylene reactor blends with tailored trimodal molar mass distributions as melt-processable all-polymer composites," Macromolecules **49**, 8048–8060 (2016).

[51] Stürzel, M., A. Kurek, M. Anselm, T. Halbach, and R. Mülhaupt, Polyolefin nanocomposites and hybrid catalysts, in *Polyolefins 50 years after Ziegler and Natta*, edited by W. Kaminsky (Springer, Heidelberg, 2013), Vols. 257–258, pp. 279–309.

[52] Kurek, A., S. Mark, M. Enders, M. Stürzel, and R. Mülhaupt, "Two-site silica supported Fe/Cr catalysts for tailoring bimodal polyethylenes with variable content of UHMWPE," J. Mol. Catal. A Chem. **383–384**, 53–57 (2014).

[53] Kurek, A., R. Xalter, M. Stürzel, and R. Mülhaupt, "Silica nanofoam (NF) supported single- and dual-site catalysts for ethylene polymerization with morphology control and tailored bimodal molar mass distributions," Macromolecules **46**, 9197–9201 (2013).

[54] Mavridis, H., and R. N. Shroff, "Temperature dependence of polyolefin melt rheology," Polym. Eng. Sci. **32**, 1778–1791 (1992).

[55] Wood-Adams, P., and S. Costeux, "Thermorheological behavior of polyethylene: Effects of microstructure and long chain branching," Macromolecules **34**, 6281–6290 (2001).

[56] Macosko, C. W., *Rheology: Principles, Measurements, and Applications* (VCH, New York, 1994).

[57] Wu, T., L. Yu, Y. Cao, F. Yang, and M. Xiang, "Effect of molecular weight distribution on rheological, crystallization and mechanical properties of polyethylene-100 pipe resins," J. Polym. Res. **20**, 271 (2013).

[58] Krishnaswamy, R. K., D. C. Rohlfing, A. M. Sukhadia, and K. R. Slusarz, "Extrusion of broad-molecular-weight-distribution polyethylenes," Polym. Eng. Sci. **44**, 2266–2273 (2004).

[59] Vinogradov, G. V., and A. I. Malkin, in *Rheology of Polymers: Viscoelasticity and Flow of Polymers*, edited by G. V. Vinogradov and A. Y. Malkin (Mir, Berlin, 1980).

[60] Stadler, F. J., C. Gabriel, and H. Münstedt, "Influence of short-chain branching of polyethylenes on the temperature dependence of rheological properties in shear," Macromol. Chem. Phys. **208**, 2449–2454 (2007).

[61] Carella, J. M., "Comments on the paper 'comparison of the rheological properties of metallocene-catalyzed and conventional high-density polyethylenes' 1," Macromolecules **29**, 8280–8281 (1996).

[62] Wasserman, S. H., and W. W. Graessley, "Prediction of linear viscoelastic response for entangled polyolefin melts from molecular weight distribution," Polym. Eng. Sci. **36**, 852–861 (1996).

[63] Derlin, S., and W. Kaminsky, "Chain-walking olefin polymerizations with donor-substituted half-sandwich chromium complexes: ethylene/propylene copolymer look-alikes by polymerization of propylene," Macromolecules **41**, 6280–6288 (2008).

[64] Trinkle, S., and C. Friedrich, "Van Gurp-Palmen-plot: A way to characterize polydispersity of linear polymers," Rheol. Acta **40**, 322–328 (2001).

[65] Fetters, L. J., D. J. Lohse, and R. H. Colby, Chain dimensions and entanglement spacings, in *Physical Properties of Polymers Handbook*, edited by J. E. Mark (Springer, New York, 2007), pp. 447–454.

[66] Larson, R. G., T. Sridhar, L. G. Leal, G. H. McKinley, A. E. Likhtman, and T. C. B. McLeish, "Definitions of entanglement spacing and time constants in the tube model," J. Rheol. **47**, 809–818 (2003).

[67] Park, J. W., J. Yoon, J. Cha, and H. S. Lee, "Determination of molecular weight distribution and composition dependence of monomeric friction factors from the stress relaxation of ultrahigh molecular weight polyethylene gels," J. Rheol. **59**, 1173–1189 (2015).

[68] van Gurp, M., and J. Palmen, "Time-temperature superposition for polymer blends," Rheol. Bull. **67**, 5–8 (1998).

[69] Nobile, M. R., and F. Cocchini, "Predictions of linear viscoelastic properties for polydisperse entangled polymers," Rheol. Acta **39**, 152–162 (2000).

[70] Milner, S. T., "Relating the shear-thinning curve to the molecular weight distribution in linear polymer melts," J. Rheol. **40**, 303–315 (1996).

[71] Likhtman, A. E., and T. C. B. McLeish, "Quantitative theory for linear dynamics of linear entangled polymers," Macromolecules **35**, 6332–6343 (2002).

[72] See supplementary material at https://doi.org/10.1122/1.5109481 for sample naming, HT-SEC traces and LVE data of multimodal PE blends. Further information is presented in the SI regarding obtained modeling parameters, MWD determined by modeling, and details concerning M_r calculation.